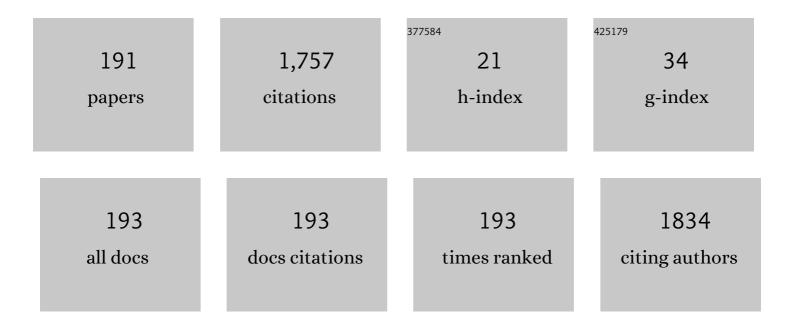
List of Publications by Year in descending order

Source: https://exaly.com/author-pdf/6659217/publications.pdf Version: 2024-02-01



#	Article	IF	CITATIONS
1	Effects of Si doping well beyond the Mott transition limit in GaN epilayers grown by plasma-assisted molecular beam epitaxy. Journal Physics D: Applied Physics, 2022, 55, 095110.	1.3	3
2	Studies on mechanical, microstructure and corrosion properties on bio-degradable Mg-Zn alloys. Materials Today: Proceedings, 2021, 37, 3550-3553.	0.9	2
3	Non-linear thermal resistance model for the simulation of high power GaN-based devices. Semiconductor Science and Technology, 2021, 36, 055002.	1.0	7
4	Source of two-dimensional electron gas in unintentionally doped AlGaN/GaN multichannel high-electron-mobility transistor heterostructures. Applied Physics Letters, 2021, 118, .	1.5	9
5	Enhanced NO <sub>2</sub> Gas Sensing Performance of Multigate Pt/AlGaN/GaN High Electron Mobility Transistors. Journal of the Electrochemical Society, 2021, 168, 047502.	1.3	7
6	Enhancement of 2D Electron Gas Mobility in an AlN/GaN/AlN Doubleâ€Heterojunction Highâ€Electronâ€Mobility Transistor by Epilayer Stress Engineering. Physica Status Solidi (A) Applications and Materials Science, 2020, 217, 1900818.	0.8	7
7	In-situ stress evolution and its correlation with structural characteristics of GaN buffer grown on Si substrate using AlGaN/AlN/GaN stress mitigation layers for high electron mobility transistor applications. Thin Solid Films, 2020, 708, 138128.	0.8	9
8	Pt/AlGaN/GaN HEMT based ammonia gas sensors. , 2019, , .		3
9	Stress optimization of AlN buffer in AlN/GaN/AlN Quantum well for DH-HEMT on SiC by PA-MBE. , 2019, ,		0
10	AlGaN/GaN HEMT-based high-sensitive NO <sub>2</sub> gas sensors. Japanese Journal of Applied Physics, 2019, 58, SCCD23.	0.8	15
11	AlGaN/GaN HEMT grown on SiC with carbon doped GaN buffer by MOCVD. , 2019, , .		6
12	Execution of julolidine based derivative as bifunctional chemosensor for Zn2+ and Cu2+ ions: Applications in bio-imaging and molecular logic gate. Spectrochimica Acta - Part A: Molecular and Biomolecular Spectroscopy, 2019, 219, 33-43.	2.0	35
13	A study on Ga Si interdiffusion during (Al)GaN/AlN growth on Si by plasma assisted molecular beam epitaxy. Applied Surface Science, 2019, 481, 319-326.	3.1	8
14	Design and Fabrication of Planar Gunn Nanodiodes Based on Doped GaN. , 2019, , .		5
15	GaN-based SSD structure for THz applications. , 2019, , .		5
16	Mid-Infrared GaN/AlGaN Quantum Cascade Detector Grown on Silicon. IEEE Electron Device Letters, 2019, 40, 263-266.	2.2	9
17	Experimental study on mechanical and corrosion characteristics of nab alloy with the addition of chromium. Materials Today: Proceedings, 2018, 5, 8089-8094.	0.9	24
18	Stress evolution of GaN/AlN heterostructure grown on 6H-SiC substrate by plasma assisted molecular beam epitaxy. AIP Advances, 2017, 7, .	0.6	4

#	Article	IF	CITATIONS
19	Quantum mechanical investigation into the electronic transport properties of a memantine-functionalized gold nanopore biosensor for natural and mutated DNA nucleobase detection. RSC Advances, 2017, 7, 8474-8483.	1.7	6
20	Study of Potential Change, Charge Distribution, Voltage Drop, Band Lineup, and Transmission Spectrum of Molecular Break Junction Under Low Bias. Journal of Physical Chemistry C, 2017, 121, 12903-12910.	1.5	3
21	GaN Schottky Metal–Semiconductor–Metal UV Photodetectors on Si(111) Grown by Ammonia-MBE. IEEE Sensors Journal, 2017, 17, 72-77.	2.4	35
22	RF reactive sputtering AlN thin film at room temperature for CMOS-compatible MEMS application. , 2017, , .		2
23	Responsivity drop due to conductance modulation in GaN metal-semiconductor-metal Schottky based UV photodetectors on Si(111). Semiconductor Science and Technology, 2016, 31, 095003.	1.0	12
24	An opto-mechanical coupled-ring reflector driven by optical force for lasing wavelength control. Applied Physics Letters, 2016, 108, .	1.5	6
25	<i>In situ</i> codoping of a CuO absorber layer with aluminum and titanium: the impact of codoping and interface engineering on the performance of a CuO-based heterojunction solar cell. Journal Physics D: Applied Physics, 2016, 49, 375601.	1.3	17
26	Characterization of highly-doped GaN as a new material for plasmonic applications. , 2016, , .		1
27	Integrated closed-loop cavity of a tunable laser. Applied Physics Letters, 2016, 109, 151105.	1.5	1
28	Optical bandgap widening and phase transformation of nitrogen doped cupric oxide. Journal of Applied Physics, 2015, 118, .	1.1	41
29	Study on GaN buffer leakage current in AlGaN/GaN high electron mobility transistor structures grown by ammonia-molecular beam epitaxy on 100-mm Si(111). Journal of Applied Physics, 2015, 117, .	1.1	6
30	Coupled-ring reflector in an external-cavity tunable laser. Optica, 2015, 2, 940.	4.8	11
31	Growth and characterization of AlGaN/GaN/AlGaN double-heterojunction high-electron-mobility transistors on 100-mm Si(111) using ammonia-molecular beam epitaxy. Journal of Applied Physics, 2015, 117, 025301.	1.1	12
32	Effect of III/V ratio on the polarity of AlN and GaN layers grown in the metal rich growth regime on Si(111) by plasma assisted molecular beam epitaxy. Japanese Journal of Applied Physics, 2015, 54, 065701.	0.8	9
33	Titanium doped cupric oxide for photovoltaic application. Solar Energy Materials and Solar Cells, 2015, 140, 266-274.	3.0	113
34	TCAD Studies on the Determination of Diffusion Length for the Planar-Collector EBIC Configuration With Any Size of the Schottky Contact. IEEE Transactions on Electron Devices, 2015, 62, 3100-3103.	1.6	4
35	<i>p</i> â€CuO/ <i>n</i> â€Si heterojunction solar cells with high open circuit voltage and photocurrent through interfacial engineering. Progress in Photovoltaics: Research and Applications, 2015, 23, 637-645.	4.4	86

An integrated tunable laser using nano-silicon-photonic circuits. , 2014, , .

#	Article	IF	CITATIONS
37	Reduction of Cu-rich interfacial layer and improvement of bulk CuO property through two-step sputtering for <i>p</i> -CuO/ <i>n</i> -Si heterojunction solar cell. Journal of Applied Physics, 2014, 116,	1.1	55
38	The study of the charge collection of the normal ollector configuration. Progress in Photovoltaics: Research and Applications, 2013, 21, 986-995.	4.4	2
39	Origin of tensile strain in GaN grown on AlGaN/AlN stress mitigating layers on 100-mm Si (111) by ammonia molecular beam epitaxy. Journal of Crystal Growth, 2013, 378, 283-286.	0.7	2
40	Strain states of AlN/GaN-stress mitigating layer and their effect on GaN buffer layer grown by ammonia molecular beam epitaxy on 100-mm Si(111). Journal of Applied Physics, 2013, 114, 123503.	1.1	8
41	Determination of Diffusion Length for the Finite Thickness Normal-Collector Configuration Using EBIC Technique. IEEE Transactions on Electron Devices, 2013, 60, 3541-3547.	1.6	4
42	Investigation on the Direct Method for the Extraction of Semiconductor Material Parameters Using the EBIC Line Scan: Planar-Collector Configuration. IEEE Transactions on Electron Devices, 2013, 60, 2346-2352.	1.6	3
43	Effect of Stress Mitigating Layers on the Structural Properties of GaN Grown by Ammonia Molecular Beam Epitaxy on 100 mm Si(111). Japanese Journal of Applied Physics, 2013, 52, 08JE05.	0.8	6
44	Demonstration of AlGaN/GaN High-Electron-Mobility Transistors on 100-mm-Diameter Si(111) by Ammonia Molecular Beam Epitaxy. Applied Physics Express, 2012, 5, 091003.	1.1	15
45	Structural properties of GaN grown on AlGaN/AlN stress mitigating layers on 100-mm Si (111) by ammonia molecular beam epitaxy. Thin Solid Films, 2012, 520, 7109-7114.	0.8	13
46	Charge collection probability: Normal-collector configuration. , 2011, , .		0
47	Improved Calculation of Charge Collection Probability From Within the Junction Well. IEEE Transactions on Electron Devices, 2011, 58, 4434-4437.	1.6	1
48	Realization of twoâ€dimensional electron gas in AlGaN/GaN HEMT structure grown on Si(111) by PAâ€MBE. Physica Status Solidi C: Current Topics in Solid State Physics, 2011, 8, 2075-2077.	0.8	4
49	Study of current collapse by quiescent-bias-stresses in rf-plasma assisted MBE grown AlGaN/GaN high-electron-mobility transistors. Solid-State Electronics, 2010, 54, 1430-1433.	0.8	7
50	Demonstration of AlGaN/GaN high-electron-mobility transistors on 100 mm diameter Si(111) by plasma-assisted molecular beam epitaxy. Applied Physics Letters, 2010, 97, 232107.	1.5	29
51	Investigation of drain current transient in BCB- and SiN-passivated Al0.25Ga0.75Asâ^•In0.2Ga0.8As pseudomorphic high electron mobility transistors. Applied Physics Letters, 2007, 90, 033501.	1.5	6
52	Surface Recombination in InP/InAlAs/GaAsSb/InP Double Heterojunction Bipolar Transistors. Indium Phosphide and Related Materials Conference (IPRM), IEEE International Conference on, 2007, , .	0.0	1
53	Evidence of Existence of Different Surface States in INP-Based High Electron Mobility Transistors (HEMTs). Indium Phosphide and Related Materials Conference (IPRM), IEEE International Conference on, 2007, , .	0.0	0
54	Current Transport Mechanism in InP/InAlAs/GaAsSb/InP Double Heterojunction Bipolar Transistors. Indium Phosphide and Related Materials Conference (IPRM), IEEE International Conference on, 2007, , .	0.0	0

#	Article	IF	CITATIONS
55	Hot-Electron-Induced Degradation in BCB- and SiN-Passivated \$hbox{Al}_{0.25}hbox{Ga}_{0.75}hbox{As/In}_{0.2}hbox{Ga}_{0.8}hbox{As}\$ PHEMTs. IEEE Transactions on Device and Materials Reliability, 2007, 7, 488-493.	1.5	3
56	Increase in electron mobility of InGaAs/InP composite channel high electron mobility transistor structure due to SiN passivation. Thin Solid Films, 2007, 515, 4387-4389.	0.8	5
57	InGaAsP/InP long wavelength quantum well infrared photodetectors. Thin Solid Films, 2007, 515, 4450-4453.	0.8	2
58	Temperature dependent study on the microwave noise performance of metamorphic InP/InGaAs heterojunction bipolar transistors. Thin Solid Films, 2007, 515, 4514-4516.	0.8	2
59	Temperature dependent microwave performance of AlGaN/GaN high-electron-mobility transistors on high-resistivity silicon substrate. Thin Solid Films, 2007, 515, 4517-4521.	0.8	53
60	Enhancement of both direct-current and microwave characteristics of AlGaNâ^•GaN high-electron-mobility transistors by furnace annealing. Applied Physics Letters, 2006, 88, 023502.	1.5	14
61	Power performance and scalability study of AlGaAs/GaAs double-recessed pseudomorphic high electron mobility transistors on unthinned substrate for coplanar waveguide circuit applications. Microelectronic Engineering, 2005, 81, 22-28.	1.1	1
62	Temperature dependence of DC and microwave characteristics of InGaAs/InP composite channel HEMTs. , 2005, , .		0
63	Microwave noise characteristics of AlGaN/GaN HEMTs on high-resistivity silicon substrate. , 2005, , .		1
64	Study of highly selective wet gate recess process for Al[sub 0.25]Ga[sub 0.75]As/GaAs based pseudomorphic high electron mobility transistors. Journal of Vacuum Science & Technology an Official Journal of the American Vacuum Society B, Microelectronics Processing and Phenomena, 2004, 22, 1653.	1.6	1
65	The Influence of Emitter Material on Silicon Nitride Passivation-Induced Degradation in InP-Based HBTs. IEEE Transactions on Electron Devices, 2004, 51, 8-13.	1.6	7
66	Thermal Resistance of Metamorphic InP-Based HBTs on GaAs Substrates Using a Linearly Graded <tex>\$hbox In_xhbox Ga_1-xhbox P\$</tex> Metamorphic Buffer. IEEE Transactions on Electron Devices, 2004, 51, 1221-1227.	1.6	34
67	Characterization of InGaAs/InP single quantum well structure on GaAs substrate with metamorphic buffer grown by molecular beam epitaxy. Journal of Crystal Growth, 2004, 261, 16-21.	0.7	11
68	A compact analytical l–V model of AlGaAs/InGaAs/GaAs p-HEMTs based on non-linear charge control model. Microelectronic Engineering, 2004, 75, 127-136.	1.1	2
69	Temperature dependence of electron ionization coefficients of InGaP measured in InGaP/GaAs/InGaP DHBT's. Journal of Crystal Growth, 2004, 268, 406-409.	0.7	Ο
70	A comparative study of metamorphic InP/InGaAs heterojunction bipolar transistors (MHBTs) grown by gas and solid source molecular beam epitaxy (MBE). Journal of Crystal Growth, 2004, 268, 410-414.	0.7	3
71	Measurements of InGaP electron ionization coefficient using InGaP-GaAs-InGaP double HBTs. IEEE Transactions on Electron Devices, 2003, 50, 1711-1714.	1.6	3
72	Temperature dependence of avalanche multiplication in inp-based HBTs with InGaAs/InP composite collector: device characterization and physics model. IEEE Transactions on Electron Devices, 2003, 50, 2335-2343.	1.6	12

#	Article	IF	CITATIONS
73	Grey scale structures formation in SU-8 with e-beam and UV. Microelectronic Engineering, 2003, 67-68, 306-311.	1.1	73
74	DC Characterization of Metamorphic InP/InGaAs Heterojunction Bipolar Transistors at Elevated Temperature. Japanese Journal of Applied Physics, 2002, 41, 1136-1138.	0.8	3
75	Studies on the Degradation of InP/InGaAs/InP Double Heterojunction Bipolar Transistors Induced by Silicon Nitride Passivation. Japanese Journal of Applied Physics, 2002, 41, 1059-1061.	0.8	17
76	Through wafer via hole by reactive ion etching of GaAs. , 2002, , .		2
77	Scaling of microwave noise and small-signal parameters of InP/InGaAs DHBT with high DC current gain. IEEE Transactions on Electron Devices, 2002, 49, 1308-1311.	1.6	4
78	InGaAs/InP single quantum well structure grown on GaAs substrate with linearly graded metamorphic InGaP buffer layer by solid source molecular beam epitaxy. Solid-State Electronics, 2002, 46, 877-883.	0.8	5
79	Growth and characterization of compositionally graded InGaP layers on GaAs substrate by solid-source molecular beam epitaxy. Journal of Crystal Growth, 2002, 243, 288-294.	0.7	7
80	Measurement and Simulation of Microwave Noise Transient of InP/InGaAs DHBT with Polyimide Passivattion. , 2001, , .		0
81	Characterization of linearly graded metamorphic InGaP buffer layers on GaAs using high-resolution X-ray diffraction. Thin Solid Films, 2001, 391, 36-41.	0.8	21
82	Optimization of compositionally graded InxGa1â^'xP metamorphic buffer layers grown by solid source molecular beam epitaxy. Materials Science in Semiconductor Processing, 2001, 4, 637-640.	1.9	7
83	Novel In0.52Al0.48As/In0.53Ga0.47As metamorphic high electron mobility transistors on GaAs substrate with InxGa1â^`xP graded buffer layers. Materials Science in Semiconductor Processing, 2001, 4, 641-645.	1.9	12
84	High-frequency performance of metamorphic InP/In0.53Ga0.47As/InP DHBT in common base configuration on GaAs substrates. Materials Science in Semiconductor Processing, 2001, 4, 647-649.	1.9	0
85	Quick derivation of high-power thermal resistance values of HBTs using an existing measurement technique and a theoretical formula. Microwave and Optical Technology Letters, 2001, 30, 287-289.	0.9	0
86	Microwave noise and power performance of metamorphic InP heterojunction bipolar transistors. IEEE Transactions on Microwave Theory and Techniques, 2001, 49, 2408-2412.	2.9	3
87	Metamorphic In[sub 0.52]Al[sub 0.48]As/In[sub 0.53]Ga[sub 0.47]As high electron mobility transistors on GaAs with In[sub x]Ga[sub 1â^x]P graded buffer. Journal of Vacuum Science & Technology an Official Journal of the American Vacuum Society B, Microelectronics Processing and Phenomena, 2001, 19, 2119.	1.6	10
88	High microwave performance of InGaP/GaAs HBT with beryllium-doped base grown by solid source MBE. , 2000, , .		0
89	Growth optimization of InGaP layers by solid source molecular beam epitaxy for the application of InGaP/In0.2Ga0.8As/GaAs high electron mobility transistor structures. Journal of Crystal Growth, 2000, 216, 51-56.	0.7	10
90	Band gap narrowing effect in Be-doped AlxGa1â^'xAs studied by photoluminescence spectroscopy. Solid-State Electronics, 2000, 44, 37-40.	0.8	7

#	Article	IF	CITATIONS
91	Optimization of InxGa1â^'xP/In0.2Ga0.8As/GaAs high electron mobility transistor structures grown by solid source molecular beam epitaxy. Materials Science and Engineering B: Solid-State Materials for Advanced Technology, 2000, 75, 110-114.	1.7	1
92	Effect of growth interruption on the electrical and optical characteristics of InP/InGaAs HEMT structures. Microelectronic Engineering, 2000, 51-52, 433-440.	1.1	1
93	Optical characterisation on the effect of doping concentration in InGaAs/InP HEMT structures. Microelectronic Engineering, 2000, 51-52, 441-448.	1.1	1
94	Electrical and optical characterization of regrown PHEMT layer structures on etched GaAs surfaces. Journal of Materials Science: Materials in Electronics, 2000, 11, 379-382.	1.1	1
95	Study of doping concentration variation in InGaAs/InP high electron mobility transistor layer structures by Raman scattering. Journal of Vacuum Science and Technology A: Vacuum, Surfaces and Films, 2000, 18, 713-716.	0.9	5
96	Preparation and characterization of rf-sputtered SrTiO3 thin films. Journal of Vacuum Science and Technology A: Vacuum, Surfaces and Films, 2000, 18, 1638-1641.	0.9	18
97	Metamorphic InP/InGaAs double-heterojunction bipolar transistors on GaAs grown by molecular-beam epitaxy. Applied Physics Letters, 2000, 77, 869-871.	1.5	45
98	Dry via hole etching of GaAs using high-density Cl[sub 2]/Ar plasma. Journal of Vacuum Science & Technology an Official Journal of the American Vacuum Society B, Microelectronics Processing and Phenomena, 2000, 18, 2509.	1.6	11
99	Electrical and optical properties of Si-doped InP grown by solid source molecular beam epitaxy using a valved phosphorus cracker cell. Journal of Applied Physics, 2000, 87, 7988-7993.	1.1	20
100	Demonstration of aluminum-free metamorphic InP/In/sub 0.53/Ga/sub 0.47/As/InP double heterojunction bipolar transistors on GaAs substrates. IEEE Electron Device Letters, 2000, 21, 427-429.	2.2	27
101	Improved transport properties of InxGa1â~'xP/In0.2Ga0.8As/GaAs pseudomorphic high electron mobility transistor structures. Solid State Communications, 1999, 112, 661-664.	0.9	2
102	Effect of acid strength of co-precipitated chromia/alumina catalyst on the conversion and selectivity in the fluorination of 2-chloro-1,1,1-trifluoroethane to 1,1,1,2-tetrafluoroethane. Journal of Fluorine Chemistry, 1999, 95, 177-180.	0.9	9
103	Reactive sputter deposition and characterization of tantalum nitride thin films. Materials Science and Engineering B: Solid-State Materials for Advanced Technology, 1999, 57, 224-227.	1.7	82
104	Characterization of beryllium doped Al0.33Ga0.67As layers grown by molecular beam epitaxy. Journal of Crystal Growth, 1999, 197, 762-768.	0.7	7
105	Characterization of silicon-doped InP grown by solid-source molecular beam epitaxy using a valved phosphorus cracker cell. Journal of Crystal Growth, 1999, 204, 275-281.	0.7	10
106	InP/InxGa1â^'xAs (0.53⩼2x⩼20.81) high electron mobility transistor structures grown by solid source molecular beam epitaxy. Journal of Crystal Growth, 1999, 207, 8-14.	0.7	4
107	Molecular beam epitaxial growth of In1â°'xâ°'yGaxAlyAs: effects of substrate temperature and V/III ratio. Materials Chemistry and Physics, 1999, 59, 20-25.	2.0	5
108	Full-wave analysis of multiconductor transmission lines on anisotropic inhomogeneous substrates. IEEE Transactions on Microwave Theory and Techniques, 1999, 47, 1764-1770.	2.9	24

#	Article	IF	CITATIONS
109	Study of Raman Scattering on InP/InGaAs/InP HEMTs. Materials Research Society Symposia Proceedings, 1999, 588, 167.	0.1	0
110	Substrate temperature effects on the growth of In1â^'xâ^'yGaxAlyAs on InP substrates by molecular beam epitaxy. Journal of Crystal Growth, 1998, 186, 315-321.	0.7	5
111	The effects of arsenic pressure on the properties of In1â^'xâ^'yGaxAlyAs layers grown by molecular beam epitaxy. Journal of Crystal Growth, 1998, 191, 24-30.	0.7	4
112	V/III ratio effects on the growth of In1â^'xâ^'yGaxAlyAs on InP substrates by molecular beam epitaxy. Microelectronics Journal, 1998, 29, 889-893.	1.1	1
113	The effects of beryllium doping in InGaAlAs layers grown by molecular beam epitaxy. Journal of Crystal Growth, 1998, 193, 285-292.	0.7	3
114	Laser excitation induced photoluminescence linewidth reduction in molecular beam epitaxial InAlAs layers grown on InP substrates. Superlattices and Microstructures, 1998, 23, 503-512.	1.4	3
115	Design and characterization of AlGaAs/InGaAs/GaAs-based double-heterojunction PHEMT device. Microwave and Optical Technology Letters, 1998, 17, 50-53.	0.9	3
116	Excitation dependence of photoluminescence linewidth in InAlAs grown on InP substrates by molecular beam epitaxy. Thin Solid Films, 1997, 295, 310-314.	0.8	1
117	Photoluminescence and raman scattering characterization of silicon-doped In0.52Al0.48As grown on InP (100) substrates by molecular beam epitaxy. Journal of Electronic Materials, 1996, 25, 1458-1462.	1.0	4
118	Mobility enhancement in MBE-grown InxGa1â^'xAs/In0.52Al0.48As modulation-doped heterostructures. Superlattices and Microstructures, 1996, 19, 159-167.	1.4	2
119	Photoluminescence and dark current of p-doped InGaAs/AlxGa1â^'xAs strained multiple quantum wells. Superlattices and Microstructures, 1996, 20, 105-110.	1.4	2
120	Molecular beam epitaxial growth of high quality InAlAs on InP (100) substrates at very high arsenic pressures. Thin Solid Films, 1996, 279, 11-13.	0.8	3
121	Silicon doping in In0.52Al0.48As layers grown by molecular beam epitaxy: characterization of material properties. Materials Science and Engineering B: Solid-State Materials for Advanced Technology, 1996, 40, 31-36.	1.7	2
122	Some effects of indium composition on pseudomorphic modulation-doped heterostructures grown by molecular beam epitaxy. Journal of Crystal Growth, 1996, 158, 443-448.	0.7	2
123	A photoluminescence and Raman scattering study of the properties of Si-doped In0.52Al0.48As grown lattice-matched to InP substrates. Journal of Materials Science Letters, 1996, 15, 311-313.	0.5	1
124	Some characteristics of silicon-doped In0.52Al0.48As grown lattice-matched on InP substrates by molecular beam epitaxy. Thin Solid Films, 1996, 287, 284-287.	0.8	3
125	On the substrate temperature dependence of the properties of In0.52Al0.48As/InP structures grown by molecular beam epitaxy. Journal of Materials Research, 1996, 11, 2158-2162.	1.2	1
126	On factors affecting alloy clustering in In0.52Al0.48As layers grown on InP substrates by molecular beam epitaxy. Superlattices and Microstructures, 1995, 17, 213-220.	1.4	3

#	Article	IF	CITATIONS
127	Some characteristics of silicon-doped In0.52Al0.48AS layers grown lattice-matched on InP substrates by molecular beam epitaxy. Superlattices and Microstructures, 1995, 17, 285.	1.4	1
128	Space charge buildup in tight-binding superlattices induced by electron sequential tunneling. Superlattices and Microstructures, 1995, 18, 83-90.	1.4	9
129	A photoluminescence and X-ray diffraction analysis of InAlAs/InP heterostructures grown by molecular beam epitaxy. Thin Solid Films, 1995, 266, 302-306.	0.8	1
130	High quality InAlAs grown on InP substrates by molecular beam epitaxy at very high arsenic overpressures. Journal of Materials Science Letters, 1995, 14, 1374-1376.	0.5	0
131	Optical and structural characterizations for optimized growth of In0.52Al0.48As on InP substrates by molecular beam epitaxy. Materials Science and Engineering B: Solid-State Materials for Advanced Technology, 1995, 35, 109-116.	1.7	3
132	Photoluminescence in degenerate p-type GaAs layers grown by molecular beam epitaxy. Materials Science and Engineering B: Solid-State Materials for Advanced Technology, 1995, 35, 449-453.	1.7	7
133	Characterization of Ni/Ge/Au/Ni/Au contact metallization on heterostructures for pseudomorphic heterojunction field effect transistor application. Materials Science and Engineering B: Solid-State Materials for Advanced Technology, 1995, 35, 234-238.	1.7	1
134	Selective wet etching of a heterostructure with citric acid-hydrogen peroxide solutions for pseudomorphic GaAs/AlxGa1â^'xAs/InyGa1â^'yAs heterojunction field effect transister fabrication. Materials Science and Engineering B: Solid-State Materials for Advanced Technology, 1995, 35, 230-233.	1.7	20
135	Characterization of beryllium-doped molecular beam epitaxial grown GaAs by photoluminescence. Journal of Crystal Growth, 1995, 148, 35-40.	0.7	35
136	Photoluminescence characteristics of Si-doped In0.52Al0.48As grown on InP substrates by molecular beam epitaxy. Journal of Crystal Growth, 1995, 151, 243-248.	0.7	1
137	Surface and electrical studies of CuO:V2O5 thin films. Thin Solid Films, 1995, 260, 161-167.	0.8	4
138	Highâ€field domain formation in GaAs/AlGaAs superlattices. Applied Physics Letters, 1995, 66, 1120-1122.	1.5	7
139	Sequential tunneling through n-type GaAs/AlGaAs multi-quantum-well structures with Schottky and ohmic contacts. Journal of Vacuum Science & Technology an Official Journal of the American Vacuum Society B, Microelectronics Processing and Phenomena, 1995, 13, 4.	1.6	13
140	The effects of Si doping in In0.52Al0.48As layers grown lattice matched on InP substrates. Journal of Applied Physics, 1995, 78, 1812-1817.	1.1	14
141	Investigation of highâ€field domain formation in tightâ€binding superlattices by capacitance–voltage measurements. Applied Physics Letters, 1995, 67, 1908-1910.	1.5	2
142	A photoluminescence study of the effect of well thickness in strained InGaAs/AlGaAs heterostructures grown by molecular beam epitaxy. Journal of Materials Research, 1994, 9, 1834-1838.	1.2	1
143	Photoluminescence studies of strained InxGa1â^xAsâ€Al0.28Ga0.72As heterostructures grown by molecularâ€beam epitaxy. Journal of Applied Physics, 1994, 76, 246-250.	1.1	10
144	Photoluminescence, intersubband absorption, and double crystal xâ€ray diffraction inpâ€doped InGaAs/AlGaAs strained multiple quantum wells. Applied Physics Letters, 1994, 65, 1430-1432.	1.5	3

#	Article	IF	CITATIONS
145	Sequential tunneling in GaAs/AlGaAs multiquantum well structures grown by molecular beam epitaxy. Journal of Applied Physics, 1994, 76, 2868-2871.	1.1	3
146	Beâ€doped GaAs layers grown at a high As/Ga ratio by molecular beam epitaxy. Journal of Vacuum Science and Technology A: Vacuum, Surfaces and Films, 1994, 12, 1120-1123.	0.9	8
147	Electrical characteristics of GaAs-Al0.33Ga0.67As tunnelling structures grown by molecular beam epitaxy. Journal of Crystal Growth, 1994, 141, 51-56.	0.7	0
148	The effect of As/Ga flux ratio on Si-doped GaAs layers grown by molecular beam epitaxy. Journal of Crystal Growth, 1994, 135, 441-446.	0.7	12
149	Effects of substrate temperature and V/III flux ratio on the growth of InAIAs on InP substrates by molecular beam epitaxy. Journal of Crystal Growth, 1994, 144, 121-125.	0.7	6
150	Indium desorption from strained InGaAs/GaAs quantum wells grown by molecular beam epitaxy. Journal of Vacuum Science and Technology A: Vacuum, Surfaces and Films, 1994, 12, 1124-1128.	0.9	13
151	Photoluminescence from strained GaAs/In0.12Ga0.88As multiple quantum-wells grown with and without growth interruption by molecular beam epitaxy. Superlattices and Microstructures, 1993, 13, 469.	1.4	2
152	Some properties of strained InxGa1-xAs/Al0.28Ga0.72As quantum well structures studied using low temperature photoluminescence. Superlattices and Microstructures, 1993, 14, 79.	1.4	2
153	On factors influencing Si segregation and its effect on the two-dimensional electron gas mobility in inverted GaAs/n-AlGaAs heterostructures. Thin Solid Films, 1993, 232, 94-98.	0.8	0
154	Optical characterization of strained InxGa1â^'xAsâ^'Al0.28Ga0.72As heterostructures grown by molecular beam epitaxy. Journal of Crystal Growth, 1993, 134, 240-246.	0.7	2
155	The effect of growth interruption on the photoluminescence linewidth of GaAs/InGaAs quantum wells grown by molecular beam epitaxy. Journal of Crystal Growth, 1993, 131, 1-4.	0.7	4
156	Some characteristics of heavily Be-doped GaAs layers grown by molecular beam epitaxy. Thin Solid Films, 1993, 235, 1-5.	0.8	6
157	The effect of interruption during the growth of strained GaAs/InGaAs/GaAs quantum wells by molecular beam epitaxy. Journal of Materials Research, 1993, 8, 3122-3125.	1.2	3
158	The diffusion coefficient of lithium in V2O5î—,2O5 and V2O5î—,TeO2 glasses. Solid State Ionics, 1992, 51, 197-202.	1.3	3
159	Fast ion conduction in Li2Oî—,GeO2î—,Nb2O5 glasses. Materials Science and Engineering B: Solid-State Materials for Advanced Technology, 1992, 14, 17-22.	1.7	2
160	Preparation and characterization of rf-sputtered thin films of Li2O-P2O5-Nb2O5 glasses. Solid State lonics, 1991, 44, 325-329.	1.3	13
161	Thin film studies on Li2O·P2O5·Nb2O5 based fast ion conducting glasses. Solid State Ionics, 1990, 40-41, 680-683.	1.3	7
162	lonic conductivity studies on Li1â^'xM2â^'xM′xP3O12 (H = Hf, Zr; M′ = Ti, Nb). Materials Research Bulletin, 1989, 24, 221-229.	2.7	39

#	Article	IF	CITATIONS
163	Electrical and electrochemical characterization of Li2O:P2O5:Nb2O5-based solid electrolytes. Journal of Non-Crystalline Solids, 1989, 110, 101-110.	1.5	70
164	Ionic conductivity studies of the vitreous Li2O:P2O5:Ta2O5 system. Journal of Non-Crystalline Solids, 1989, 108, 323-332.	1.5	33
165	Mixed cationic effect in the Li/Agî—,B2O3î—,P2O5 glasses. Solid State Ionics, 1987, 24, 81-88.	1.3	4
166	Ionic transport studies of solid electrolytes using microcomputer controlled instrumentation. Solid State Ionics, 1987, 24, 225-233.	1.3	16
167	Fatigue and Reliability Evaluation of Unnotched Carbon Epoxy Laminates. Journal of Composite Materials, 1984, 18, 21-31.	1.2	26
168	High field domain formation and current-voltage hysteresis in selectively doped GaAs/AlGaAs multiple-quantum-well structures. , 0, , .		0
169	Some characteristics of mobility enhancement in pseudomorphic In/sub x/Ga/sub 1-x/As/In/sub 0.52/Al/sub 0.48/As/InP high electron mobility transistor structures. , 0, , .		0
170	High linearity, current drivability and f/sub max/ using pseudomorphic GaAs double-heterojunction HEMT (DHHEMT). , 0, , .		0
171	Excitation dependence of photoluminescence linewidth in InAlAs grown on InP substrates by molecular beam epitaxy. , 0, , .		Ο
172	An efficient iterative solver for the modes in a dielectric waveguide. , 0, , .		2
173	Efficient analysis of microstrip structures with multiple discontinuities. , 0, , .		1
174	Metamorphic InP/InGaAs double-heterojunction bipolar transistor structure grown on GaAs by solid source molecular beam epitaxy. , 0, , .		1
175	Device performance and transport properties of high gain metamorphic InP/InGaAs heterojunction bipolar transistors at elevated temperature. , 0, , .		1
176	Microwave noise and power performance of metamorphic InP heterojunction bipolar transistors (HBTs). , 0, , .		0
177	Ammonia (NH/sub 3/) plasma surface passivation of InP/InGaAs heterojunction bipolar transistors. , 0, , .		0
178	Microwave noise and small-signal parameters scaling of InP/InGaAs DHBT with high DC current gain. , 0, , .		0
179	Understanding the degradation of InP/InGaAs heterojunction bipolar transistors induced by silicon nitride passivation. , 0, , .		4
180	A comparative study of silicon nitride passivation on InP-based double heterojunction bipolar transistors (DHBTs) with different emitter structures. , 0, , .		0

#	Article	IF	CITATIONS
181	Metamorphic InP/InGaAs heterojunction bipolar transistors under high-current and high temperature stress. , 0, , .		1
182	Temperature-dependent breakdown behavior in InP double heterojunction bipolar transistors (DHBTs) with InGaAs/InP composite collector. , 0, , .		0
183	On the thermal resistance of metamorphic and lattice-matched InP HBTs: a comparative study. , 0, , .		4
184	High breakdown voltage In/sub 0.52/Al/sub 0.48/As/In/sub 0.53/Ga/sub 0.47/As metamorphic HEMT using In/sub x/Ga/sub 1-x/P graded buffer. , 0, , .		1
185	Theoretical and experimental investigation of temperature-dependent avalanche multiplication in InP-based heterojunction bipolar transistors with InGaAs/InP composite collector. , 0, , .		1
186	Low-frequency noise characterization of metamorphic InP/InGaAs heterojunction bipolar transistors on GaAs substrate. , 0, , .		0
187	Investigation of drain current transient in InP-based high electron mobility transistors (HEMTs). , 0, , .		2
188	Device stability of metamorphic InP/InGaAs heterojunction bipolar transistors by optical and electrical characterization. , 0, , .		0
189	Characterization of mosaic structures in metamorphic inp layers grown on GaAs substrate by solid source molecular beam epitaxy. , 0, , .		Ο
190	RF performance and microwave noise of metamorphic InP/InGaAs heterojunction bipolar transistors at elevated temperature. , 0, , .		0
191	High Frequency Drain Noise in InAlAs/InGaAs/InP High Electron Mobility Transistors in Impact Ionization Regime. , 0, , .		2